

Short-term morphodynamic changes in a fetch limited beach at the Ebro delta (Spain), under low wave-energy conditions

C. Mösso†, J. P. Sierra†, V. Gracia†, M. Mestres† and A. Rodriguez‡

†Laboratori d'Enginyeria Marítima, Universitat Politècnica de Catalunya, 08034 Barcelona, Spain.
cesar.mosso@upc.edu

† Centre Internacional d'Investigació dels Recursos Costaners, Jordi Girona 1-3, Edifici D1 Campus Nord, 08034 Barcelona, Spain.

‡ Facultad de Ciencias Exactas, Físicas y Naturales, Universidad Nacional de Córdoba. Av. Vélez Sarsfield 1601, (Sede Ciudad Universitaria), Córdoba, Argentina. arodrig@com.uncor.edu



ABSTRACT

Mosso, C., Sierra, J. P., Gracia, V., Mestres, M., and Rodriguez, A. 2011. Short-term morphodynamic changes in a fetch limited beach at the Ebro delta (Spain), under low wave-energy conditions. *Journal of Coastal Research*, SI 64 (Proceedings of the 11th International Coastal Symposium), 3: 7 – 3: ; . Szczecin, Poland, ISSN 0749-0208

Sandy beaches in fetch-limited environments are protected from large ocean-generated swell waves, and fetch characteristics allow local wind-generated waves and currents to develop and drive the main morphodynamic processes. The morphodynamics of these low-energy beaches present a peculiar behaviour since there is not a dominant forcing mechanism inducing the beach changes. The main objective of this work is to describe and quantify the observed morphodynamic changes at the barred, quasi longshore-uniform beach of the Trabucador Bar at the Ebro Delta (Spain) under low-energy conditions. A nine-day field campaign was carried out within the framework of the European project FANS (Fluxes Across Narrow Shelves. The Ebro Delta Case) supported by the EC MAST-III Research Programme, (Contract No. MAS3-CT95-0037, DG12 – ESCY) and the measurements included a detailed topo-bathymetric surveying at the beginning and at the end of the campaign, video recordings covering the whole domain of the study area, surf zone waves and currents time series obtained at different positions and depths, nearshore pressure and horizontal velocities time series outside the surf zone. The results show that the beach underwent important longshore and cross-shore (the breaching of the submerged bar) morphodynamic changes under low-energy conditions. The observations suggest that the low-energy wave field and the beach profile played a key role in the generation of low frequency oscillations and rip currents that reshaped the whole study zone.

ADDITIONAL INDEX WORDS: *Fetch limited beaches, coastal morphodynamics, field measurements, Ebro Delta*

INTRODUCTION

The littoral area presents a series of dynamic phenomena such as waves, currents, wave-current interaction and sediment transport. Within this area, the most active region is the surf zone, which can be characterized by high energy dissipation rates, complex circulation patterns (Rodriguez *et al.*, 2001) and sediment movement that result in bottom topography variations and the morphodynamic evolution of the beach.

A major modifying agent, in terms of both morphology and sand volume, are storms (Lee *et al.*, 1998, Hill *et al.*, 2004). Under these highly energetic events, sand tends to be transported rapidly offshore, as opposed to low-energy episodes that transport sediment onshore, causing gradual beach accretion.

Wright and Short (1984) and Lippmann and Holman (1990), among others, described the morphology of a beach as a function of the incoming waves and derived hydrodynamics and the existing sediment characteristics. Their models report the creation of a bar (offshore sediment transport) after the pass of a storm and its welding to the shore when the incoming energy diminishes indicating a clear onshore movement.

Because of the coastal impact of storms, many studies analyze the evolution of beach morphodynamics under high energy conditions. Cooper and Jackson (1999) showed that the alongshore transport during storms often exceeds non-storm rates by several orders of magnitude. Seymour *et al.* (2005) analyzed

the evolution of a beach fill in California under a storm with a maximum significant wave height H_s of 3.2 m, and found that the mean erosion was of about 145 m³/linear meter, and it was not alongshore-uniform. In contrast to this, beach morphodynamics under low-energy conditions remain poorly studied. Different studies (Ekwurzel, 1990; Guillén and Palanques, 1996; Hegge *et al.*, 1996; Goodfellow and Stephenson, 2005) indicate that low-energy beaches exhibit variable behaviour and do not necessarily conform to Wright and Short's (1984) morphodynamic model.

According to Jackson *et al.* (2002), low-energy beaches occur where non-storm wave heights are very small (e.g. less than 0.25 m), and H_s during strong onshore winds are small (e.g. less than 20 m in microtidal environments), and morphological features are inherited from higher-energy events. Jackson *et al.* (2002) also stated that there is little cross-shore sediment exchange on low-energy beaches. Moreover, Goodfellow and Stephenson (2005) pointed out that low-energy beaches are located in sheltered and/or fetch-limited environments.

The present paper analyzes the short term morphodynamic evolution of a stretch of the Trabucador beach, located in the Ebro Delta. The aim of this study is, firstly, to examine the morphodynamic behaviour of this beach under low-energy conditions and, secondly, to determine if these can lead to significant variations in the beach topography. Observations used

in the analysis were obtained during a field campaign carried out under low-energy conditions (Mösso *et al.*, 2002). During this field campaign, besides topographic surveys, wind, wave and current data were recorded by means of a series of devices deployed in the studied area. Hence, interaction between hydrodynamics and morphodynamics is examined.

STUDY AREA

The Ebro Delta is located on the Spanish Mediterranean coast (Fig. 1). It is a 50 Km-long sandy shoreline developed during the last five centuries by the sediment supplied by the Ebro river. At present, the delta can be classified as a wave-dominated type due to the drastic reduction of the river sand supply originated by the construction of several dams along its course (Sierra *et al.*, 2004).

As most of the Mediterranean coast, the Ebro delta area is a microtidal environment, with a maximum astronomical tidal range of 0.25 m (López *et al.*, 1992). On the other hand, storm surges are an important dynamic agent in the area, having the same order of magnitude than the astronomical oscillations and, in extreme events, exceeding them by 500% originating maximum sea level rises of about 1 m. In this area, the prevailing winds during the summer blow from the S and SW direction, although the strongest come from the E. During winter, the most frequent winds blow from the NW (Sierra *et al.*, 2004). On the other hand, the incident waves on the Ebro delta come basically from three directions: E-NE, S and NW (García *et al.*, 1993). The average offshore H_s is 0.75 m, the mean wave period is 3.9 s and the peak period is 5 s. Nearly all the mean wave periods have values between 2 and 8 s. The maximum peak period during storms is of about 11 s.

The presence of two spits in the Ebro delta indicate a net longshore sediment transport directed towards the south in the southern hemidelta and towards the north in the northern part of the delta (Guillén and Jiménez, 1995). The main morphological features along the coast are longshore bar-and-trough systems, which are present throughout all the year, although they change as a function of energetic conditions (Gracia, 2005).

METHODS

A field campaign was carried out in the Ebro Delta area from October 30th to November 10th, 1996, to study surf zone processes. The experiments were focused on the nearshore area, from the

shoreline to a depth of about 3 m and were done at the Trabucador bar, in the southern hemidelta (Fig. 2). The selected coast corresponds to a sandy beach with fine sand ($d_{50} \approx 0.2$ mm), almost longshore-uniform and with submerged bars, which are parallel to the coast.

The field campaign included detailed and simultaneous measurements of topo-bathymetry, meteorology, hydrodynamics and sediment transport, both inside and outside the surf zone. The bathymetry (12 beach profiles) was measured before (30/Oct) and after (09/Nov) the hydro-morphodynamic field campaign, using conventional topography. Each point of the profiles was taken by direct radiation to a maximum depth of 2 meters using conventional instruments. For the whole topo-bathymetric survey, a total of 1248 points were measured, distributed over 12 cross-shore profiles located at $x = -140, -90, -40, -20, -10, 0, 10, 20, 40, 60, 110$ and 140 m (in longshore local coordinates) and 90 m (in cross-shore local coordinates). Only profiles at $x = -10, 0$ and 10 were extended up to 170 m cross-shore. The profiles in the central part had a separation of 10 and 20 m, while those located at the outer zone of the measuring area had a separation of 50 m.

The field survey was referenced to a local coordinate system with the horizontal axis parallel to the coast orientation and the origin of coordinates centred in the working area of the sledge. The data were later linked to the UTM projection system and Catalan geoid GEOID'91.

Outside the surf zone, hydrodynamic data were acquired with an Interocean S4DW currentmeter located at a depth of 2 m and installed on a tetrapod moored at the 3.5 m isobath. The S4DW had a pressure sensor (allowing waves and water levels to be recorded) and a biaxial electromagnetic currentmeter that measured horizontal currents. Waves were measured for 35 minutes every hour with a sampling rate of 2 Hz. Water levels and currents were obtained every 30 minutes by averaging 2-minute time series sampled with a frequency of 2 Hz. Offshore wave data were also measured by a directional Waverider buoy located off Tortosa Cape, approximately at -50 m depth. Meteorological data (temperature, atmospheric pressure and wind velocity and direction) were recorded by a nearby Aanderaa meteorological station, located at an altitude of 10 m.

Inside the surf zone, the hydrodynamic observations included 49 tests (from 02/Nov to 09/Nov) measuring waves, water levels and current velocities with an Etrometa E46400 wave-gauge and 6 Delft P-EMS-S electromagnetic currentmeters. The wave gauge acquired data at a frequency of 4 Hz. Five currentmeters were placed at 5, 10, 25, 65 and 100 cm from the bottom, measuring horizontal velocities (components in x and y directions) at a frequency of 20 Hz. The sixth currentmeter was also placed at 65 cm from the bottom, but with a different orientation to measure 2 DV velocities (components in x and z directions). All the sensors were mounted on a movable sledge, whose location changed during the experiments yielding 45 different positions (figure 2). The duration of the recorded time series was of 30 minutes.

Simultaneously to the hydrodynamic measurements from the sledge, lagrangian buoys and dye tracers were released in order to estimate turbulent diffusion coefficients. The measurements were completed by recording video images with a camera suspended from a crane at 40 m above the sea surface. These video images were processed with the DigImage software (developed by the CERC and the Cambridge University) to obtain quantitative information about waves and currents characteristics, and dye tracer dispersion.

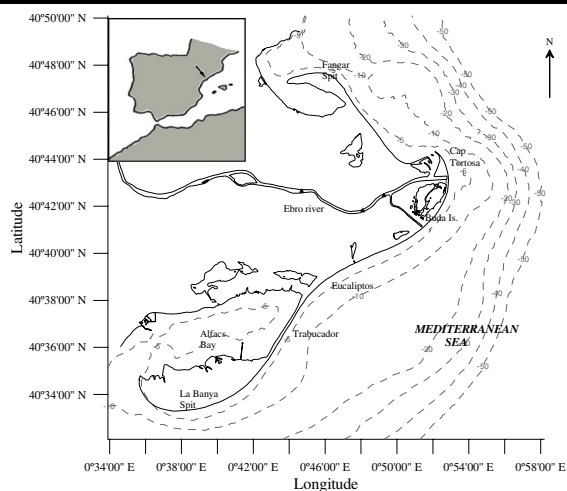


Figure 1. Study Area. Ebro Delta and location of the Trabucador bar where the field campaign was carried out.

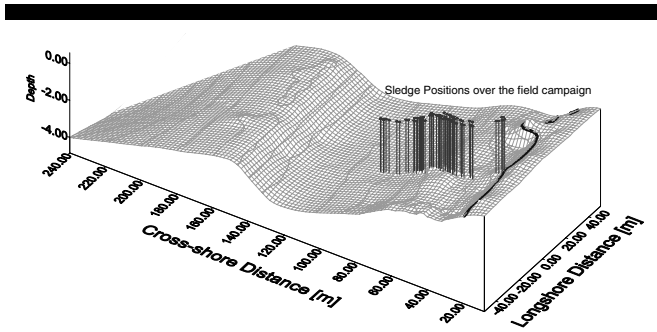


Figure 2. Sledge positions during the Delta'96 experiments and initial bathymetry (in local coordinates).

RESULTS

Meteorology and Hydrodynamics

The Delta'96 campaign was conducted during autumn, when storms are more frequent and more energetic in this part of the Mediterranean Sea. Nevertheless, the presence of an unexpected anticyclone led to low energetic conditions during almost the whole campaign, with the exception of one day (05/Nov). Time series of the meteorological conditions and hydrodynamic parameters recorded during the survey are presented in figure 3. It can be observed that winds were weak during almost all the campaign, showing diurnal variations which indicate a breeze regime. The velocities ranged between 1 to 6 m/s, except on 05/Nov, when velocities larger than 12 m/s were recorded.

The atmospheric pressure (figure 3a) reached the highest values during the first days of campaign, oscillating between 1020 and 1025 mbar and suddenly dropping on 04/Nov, reaching a minimum of 1008 mbar in the morning of 05/Nov and then rising

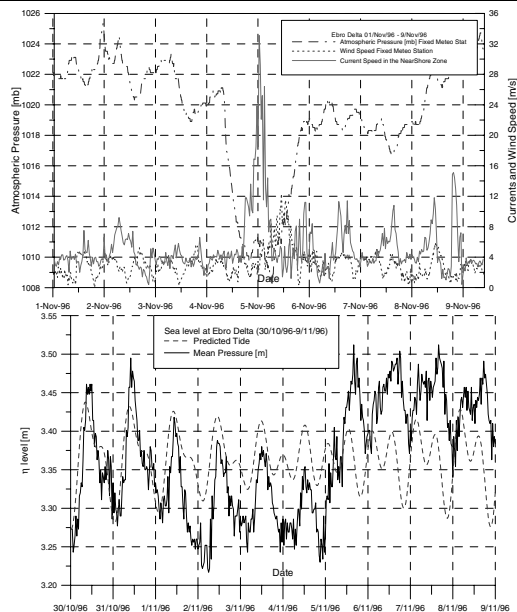


Figure 3. Atmospheric Pressure, Wind Speed and Nearshore Currents measured along the field campaign (a) and free surface measured at -3.5 m depth, compared to the predicted tide (b).

again to values around 1020 mbar on the days after. Recorded variations of mean water level during the survey period showed a mixed tidal fluctuation typical of the study area with dominance of the diurnal component. The amplitude of the oscillations decreased from 17 cm on 01/Nov to 11 cm on 04/Nov, when neap tide took place. After this day, the tidal amplitude started to increase again (figure 3b). Together with these tidal oscillations, the mean water level experienced a sudden rise during 05/Nov, associated to the atmospheric pressure drop. This pressure-induced sea level rise was of the same order of magnitude than tidal oscillations (about 17 cm). Once the atmospheric pressure rose again to high values, the sea level remained high, following only tidal oscillations.

The longshore and cross-shore velocities measured in the surf zone (averaged over 5-minute periods) were analyzed to find the minimum and maximum wave energy during each 30-minute test (see fig 4). For this analysis, only the permanently submerged currentmeters were used. The results for the test carried out during 05/Nov (when the nearshore wind-induced currents were stronger) show that, for significant breaking wave height (H_{sb}) of 40 cm or less, the vertical profile of the longshore current was quite homogeneous and with low velocities. In these conditions, the longshore current ranged from 0.12 cm/s (southward, at 10 cm from the bottom, test 0502) to 3.36 cm/s (northward, at 25 cm from the bottom, test 0503). However, under more energetic conditions, with H_{sb} of 60 cm, the longshore velocity profile showed a curved shape, with maximum velocities at 65 cm from the bottom. The values ranged from 13.56 cm/s (southward, at 10 cm from the bottom, test 0509) to 23.5 cm/s (southward, at 65 cm from the bottom, test 0508). Regarding the cross-shore velocities, under low-energy conditions, they ranged from 0.30 cm/s (seaward, at 65 cm from the bottom, test 0505) to 5.45 cm/s (seaward, at 5 cm from the bottom, test 0502) and under higher energy conditions, from 8.61 cm/s (seaward, at 1 m from the bottom, test 0506) to 23.48 cm/s (seaward, at 65 cm from the bottom, test 0508). Under low-energy conditions, the less-defined longshore current presented some changes in flow direction close to the bottom, while at higher energy conditions, this was not observed. The cross-shore currents showed a typical velocity profile with onshore currents in the upper part of the water column (due to the wave mass flux), and significant velocity values close to the bottom, indicating the presence of intense undertow fluxes. Even under low-energy conditions, the maximum velocity gradients in the surf zone were observed in undertow flow profiles in the first 5 cm above the bottom, with values ranging from 0.64 $\text{cm}\cdot\text{s}^{-1}/\text{cm}$ (test 0503) to 2.51 $\text{cm}\cdot\text{s}^{-1}/\text{cm}$ (test 0509). Nevertheless,

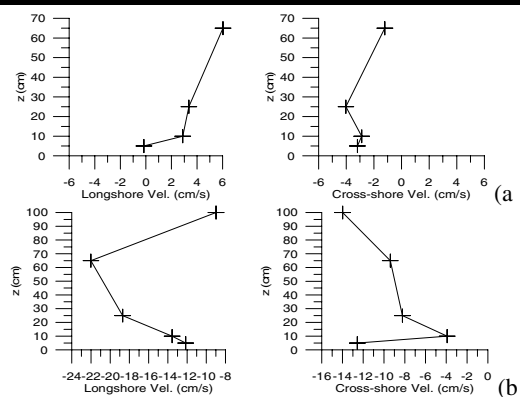


Figure 4. Longshore and cross-shore velocities, tests 0503 (low wave-energy) and 0509 (high wave-energy conditions).

as expected, the depth-averaged longshore currents were more intense than the cross-shore ones. An example of longshore and cross-shore current profiles under low and high wave energy conditions can be seen in figure 4 (negative values in longshore and cross-shore currents indicate southward and seaward flow respectively).

Bathymetric changes and morphodynamics

The initial bathymetric survey showed the presence of two submerged bars at approximately 45 m (less evident) and 130 m (at a depth of 1.5 m) from the shoreline (figure 5). Changes in the bathymetry have been calculated by direct comparison of the twelve beach profiles measured on 30/Oct and 09/Nov. According to the difference between the initial and final profiles, up to 90 m in the cross-shore direction, in 8 out of 12 (at $x = -130, -90, 10, 0, 10, 20, 40$ and 140 m), the final stage resulted in a net beach erosion, being much more intense in the central part of the study zone (profiles at $x = 10$ and 40 m). Only some accretion was observed in profiles at $x = -40$ and -20 m and at $x = 60$ and 110 m, (northward and southward of the most eroded zone respectively). However, considering the complete central profiles (up to 170 m offshore), the final stage shows a net accretion at the profile, since in the deeper zone there was a net accumulation.

In order to quantify the beach evolution during the Delta'96 field campaign, the profiles were extrapolated using a simple linear triangulation method. In the initial stage, the presence of a cusp between profiles at $x = 20$ and 40 m and the somewhat longshore uniformity of the first submerged bar stand out. In the final stage, some significant changes in the shoreline and bottom configuration appear. After the experiments, the shoreline presented a smoother configuration with no beach cusps at all. But more noticeable is the significant sand loss of the inner bar, and also its final form, since erosion patterns presented a seaward

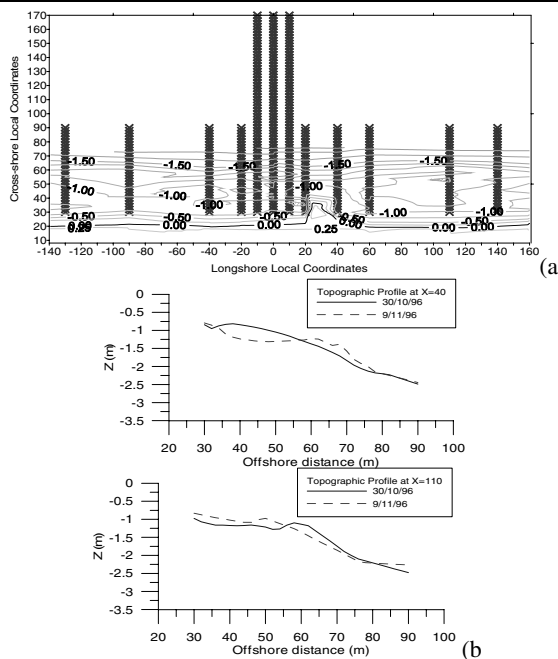


Figure 5. Topo-bathymetric survey and location of each cross-shore transects (a). Comparison of the initial and final beach profiles of the two transects that showed the most significant changes ($x=40$, erosion and $x=110$, accretion, respectively) (b).

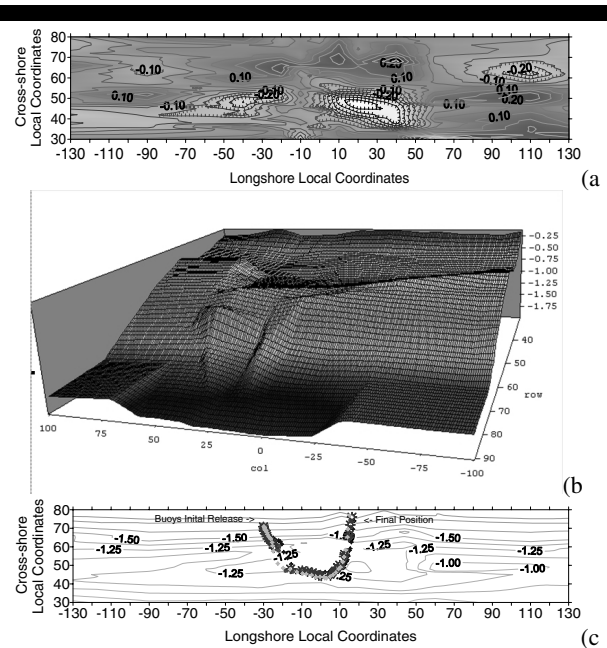


Figure 6. Erosion (light) and accretion (dark) patterns during the field experiments (a) and Breached bar and a well developed rip channel over which the lagrangian buoys drifted (b)

curved shape at both sides of the eroded zone. Here, the maximum negative depth differences (erosion) reached 45 cm between profiles at $x = 20$ and 40 m., and between $y = 35$ and 55 m (approximately between $h = 0.5$ and 0.6 m depth of the initial bathymetry). This is also observed northward of the central part, though the change ratio is smaller. Between profiles $x = -130$ and -90 m, the highest erosion rate was observed between 5 and 10 m seaward of the shoreline, and between profiles $x = -90$ and -20 m, this erosion was enhanced and the erosion pattern in the inner bar started to deflect towards the sea. Though with different erosion rates, similar mirror-type behaviour was observed southward of the central part, with the inner bar getting a curved shape pointing seaward. While close to the shoreline, the net evolution in the central part of the study zone lead to erosion, in the deeper part of these profiles, at approximately 15 m from the former shoreline, and between profiles $x = -40$ and 40 m, there was a net sand accumulation, up to 32 cm. The opposite behaviour was observed between the profiles at $x = 60$ and 140 m, where there was a net sand accumulation close to the shoreline, and erosion in the deeper part of those profiles.

The final stage of the beach shows not only the breach of the inner bar, but also a well defined cross-shore channel, not present in the initial bathymetry (figure 6). This channel was produced by a cell system circulation pattern, in which a rip current was identified from the path followed by 4 lagrangian buoys released close to the inner bar during the final test of the Delta'96 field campaign. The recorded buoy path described 3 well differentiated episodes. First, the buoys followed a shoreward trajectory during approximately the first 15 minutes after release, in a clear diagonal path (≈ 30 m), followed by a well-defined longshore trajectory (though with a slight onshore component) during 5 minutes (≈ 21 m) and finally a well-defined seaward trajectory, clearly following the abovementioned channel crossing the inner bar (≈ 38 m) during 5 minutes. The onshore velocities reached 65 cm/s and the offshore velocities reached 70 cm /s. The observed longshore velocities reached 35 cm/s

SUMMARY AND CONCLUSIONS

In this study, the morphological changes under low-energy conditions at the Trabucador Bar during the Delta'96 field campaign were assessed, along with the hydrodynamic forcing mechanisms, by analyzing a wide range of topo-bathymetric data and wind speed, currents and wave height measurements. During the field experiments, the wind presented a weak breeze regime, with velocities of 1 to 6 m/s, except for one day, when the wind speed exceeded 12 m/s. Atmospheric pressure during the first days of campaign showed high values, oscillating between 1020 and 1025 mbar. During 04/Nov, the atmospheric pressure suddenly dropped, reaching a minimum of 1008 mbar in the 05/Nov morning and then rose again to values around 1020 mbar. Most of the time, the observed H_s was smaller than 40 cm. The wave induced longshore currents under low wave energy presented a homogeneous profile, in which the only important velocity gradients were observed close to the bottom. When H_s exceeded 60 cm, the longshore profiles showed a curved shape, with larger velocity gradients in the water column, and maximum velocities (23.5 cm/s) measured at 65 cm from the bottom. Regarding the cross-shore velocity profiles, in most of the cases, there was an upper onshore component due to wave breaking, and a bottom seaward component, with maximum velocities close to the bed due to the undertow. Although the depth-averaged longshore currents were stronger than the cross-shore flows, the strongest velocity gradients were observed close to the bottom in the seaward flux. The related morphodynamic changes of the studied area (analyzed through the bathymetric changes at each profile) presented, in general, a slight erosion in the shallower zones of the beach at the northern and southern ends of the beach, and a more intense erosion in the centre. However, extending the length of the central profiles, the beach evolution results in a net accretion, suggesting that the eroded sediment from the shallower zone was transported to deeper waters by the intense undertow fluxes measured during the field campaign. Moreover, the final stage of the central part of the beach after the experiments showed a peculiar configuration with the breaching of the inner bar and the presence of a cross-shore channel. The trajectories of a set of 4 lagrangian buoys, released during the last field test revealed the presence of an intense rip current, with surface velocities close to 70 cm/s, flowing exactly through the aforementioned channel. The low wave energy conditions, the beach slope ($\tan \beta \approx 0.027$) and the small wave incidence angle during these field experiments may have induced the presence of edge waves, longshore variations in breaker heights and a concomitant longshore gradient in the water level in the surf zone, capable of generating a cell circulation system. This, together with the intense undertow fluxes, resulted in a net seaward flux of water and sediment, eroding the inner bar and generating a well defined rip channel.

LITERATURE CITED

- Cooper, J.A.G., and Jackson, D.W.T., 1999. Wave spray-induced sand transport and deposition during a coastal storm, Magilligan Point, Northern Ireland. *Marine Geology* 161, 377-383.
- Ekwurzel, B., 1990. A complex bayside beach: Herring Cove beach, Cape Cod, Massachusetts, USA. *Journal of Coastal Research* 6, 879-891.
- García, M.A.; Sánchez-Arcilla, A.; Sierra, J.P.; Sospedra, J., and Gómez, J., 1993. Wind waves off the Ebro Delta, NW Mediterranean. *Journal of Marine Systems* 4, 235-262.
- Goodfellow, B.W., and Stephenson, W.J., 2005. Beach morphodynamics in a strong-wind bay: a low-energy environment? *Marine Geology* 214, 101-116.
- Gracia V. 2005. Dinámica sedimentaria en la plataforma interna del delta del Ebro. Ph. D Thesis. Catalonia Univ. Technol. Barcelona.
- Guillén, J., and Jiménez, J.A., 1995. Processes behind the longshore variation of the sediment grain size in the Ebro Delta coast. *Journal of Coastal Research* 11, 205-218.
- Guillén, J., Palanques, A., 1996. Short and medium term grain size changes in deltaic beaches (Ebro delta, NW Mediterranean). *Sedimentary Geology* 101, 55-67.
- Hegge, B.; Eliot, I., and Hsu, J., 1996. Sheltered sandy beaches of southwestern Australia. *Journal of Coastal Research* 12, 748-760.
- Hill, W.H.; Kelley, J.T.; Belknap, D.F., and Dickson, S.M., 2004. The effects of storms and storm-generated currents on sand beaches in Southern Maine, USA. *Marine Geology* 210, 149-168.
- Jackson, N.L.; Nordstrom, K.F.; Eliot, I., and Masselink, G., 2002. Low-energy sandy beaches in marine and estuarine environments: a review. *Geomorphology* 48, 147-162.
- Lee, G.; Nicholls, R.J., and Birkemeier, W.A., 1998. Storm-driven variability of the beach- nearshore profile at Duck, North Carolina, USA, 1981-1991. *Marine Geology* 148, 163-177.
- Lippmann, T.C., and Holman, R.A., 1990. The spatial and temporal variability of sand bar morphology. *Journal of Geophysical Research* 95, 11575-11590.
- Lopez, O., Garcia, M.A., Gracia, V., 1992. Analisis y propuesta de soluciones para estabilizar el Delta del Ebro: Estudio de las variaciones del nivel del mar a partir de 10s registros de marea en L'Ametlla de Mar. Tech. Rep. LT-3/6, Generalitat de Catalunya. Barcelona.
- Mösso, C.; Sánchez-Arcilla, A., Madsen, O., Sierra, J.P., and Cáceres, I., 2002. Another approach to longshore current evaluation. *Proc. 28th International Conference on Coastal Engineering*, pp. 877-884
- Rodriguez, A.; Mösso, C.; Sierra, J.P.; Sánchez-Arcilla, A., and Collado, F., 2001. Corrientes longitudinales y resistencia al flujo en zona de rompientes. *Ingeniería Hidráulica en México* 16, 35-43.
- Seymour, R.; Guza, R.T.; O'Reilly, W., and Elgar, S., 2005. Rapid erosion of a small southern California fill. *Coastal Engineering* 52, 151-158.
- Sierra, J.P.; Sánchez-Arcilla, A.; Figueras, P.A.; González del Río, J.; Rassmusen, E.K., and Mösso, C., 2004. Effects of discharge reductions on salt wedge dynamics of the Ebro river. *River Research and Applications* 20, 61-77.
- Wright, L.D., and Short, A.D., 1984. Morphodynamic variability of surf zones and beaches: a synthesis. *Marine Geology* 56, 93-118.

ACKNOWLEDGEMENTS

These experiments were done within the framework of the FANS (MAS3-CT95-0037) projects of the UE's MAST program, CIIRC and MEC's DGICYT (CE94-0022) projects. The authors want to thank all of them who endured the field work: M. Diez, N. Pykhov, O. Pushkarev, I. Podymov, I. Rodriguez, B. Mercader, J.A. García, F. Nieto, P. Medina, C. Gallimani, E. Bahía, J.M. Redondo, J. Gómez, J. Pablo, M. Garrido, A. Caballero, Q. Sospedra and A. Chalera, amongst others.